

MORPHOLOGICAL PECULIARITIES OF REGENERATION OF ORAL MUCOSA ASSOCIATED WITH USE OF POLYMERIC PIEZOELECTRIC MEMBRANES

Koniaeva AD¹✉, Varakuta EYu¹, Leiman AE¹, Rafiev DO¹, Bolbasov EN², Stankevich KS³

¹ Human anatomy department, General medicine faculty, Siberian State Medical University, Tomsk, Russia

² National Research Tomsk Polytechnic University, Tomsk, Russia

³ Chemistry and biochemistry faculty, Montana State University, Bozeman, MT, USA

Wound defects of the oral mucosa are a common pathology the treatment of which often involves synthetic membranes. Development of varieties of such membranes is an ongoing process. This study aimed to register morphological features of the oral mucosa regeneration process in the presence of one of the varieties, the polymer piezoelectric membranes. The study involved 45 Wistar rats divided into 3 groups: 1) animals with an open wound defect; 2) animals with a wound defect covered with a copper-coated polymer membrane; 3) intact animals. The samples for morphometric study were collected on the 3rd, 7th and 12th days. On the 3rd day, rats of group 1 had the specific area of granulation tissue 1.4 times greater than that in group 2 ($p = 0.033$). In group 1 rats, endotheliocytes expressed more VEGF than in the animals of group 2. In group 2, the defect was ultimately completely covered with the epithelial layer, which was not the case in group 1. On the 7th day, the epithelium in rats of group 2 was twice as thick as the layer registered in group 1 ($p = 0.019$). Granulation tissue was replaced by loose fibrous connective tissue. In group 1, the specific area of inflammatory infiltration was greater than that of loose fibrous connective tissue, and the VEGF expression level was lower than in group 2. On the 12th day, the predominant tissue in group 2 was the loose fibrous connective tissue, the VEGF expression level equaled that of group 3, and peripheral nerves began to grow. In group 1, the specific area of dense fibrous tissue was 3.9 times greater than that in group 2 ($p = 0.012$), the epithelium had pathological changes and the VEGF expression was below control values. Thus, a polymer piezoelectric membrane had a positive effect on the post-wound restoration of the oral mucosa tissues.

Keywords: regeneration, wound defect, scaffolds, piezoelectrics, oral mucosa, inflammation

Funding: the study was supported by the Russian Foundation for Basic Research under research project №23-25-00346.

Author contribution: Koniaeva AD, Varakuta EYu, Bolbasov EN, Stankevich KS — study concept and design; Koniaeva AD, Leiman AE — collection and processing of the material; Koniaeva AD, Varakuta EYu, Rafiev DO — text authoring; Koniaeva AD, Varakuta EYu, Rafiev DO, Bolbasov EN, and Stankevich KS — text editing.

Compliance with ethical standards: the study was approved by the Ethics Committee of the Siberian State Medical University (Minutes № 7693/1 of August 26, 2019). All manipulations with the animals were done as prescribed by the Directive 2010/63/EU of the European Parliament of September 22, 2010 "On the protection of animals used for scientific purposes", and the Declaration of Helsinki.

✉ **Correspondence should be addressed:** Anastasiia D. Koniaeva
Moskovsky Trakt, 2, Tomsk, 634034, Russia; asyakonya95@gmail.com

Received: 18.05.2023 **Accepted:** 02.06.2023 **Published online:** 19.06.2023

DOI: 10.24075/brsmu.2023.020

МОРФОЛОГИЧЕСКИЕ ОСОБЕННОСТИ РЕГЕНЕРАЦИИ СЛИЗИСТОЙ ОБОЛОЧКИ ПОЛОСТИ РТА ПРИ ПРИМЕНЕНИИ ПОЛИМЕРНЫХ ПЬЕЗОЭЛЕКТРИЧЕСКИХ МЕМБРАН

А. Д. Коняева¹✉, Е. Ю. Варакута¹, А. Е. Лейман¹, Д. О. Рафиев¹, Е. Н. Больбасов², К. С. Станкевич³

¹ Сибирский государственный медицинский университет, Томск, Россия

² Томский политехнический университет, Томск, Россия

³ Государственный университет штата Монтана, Бозмен, Монтана, США

Раневые дефекты слизистой оболочки рта являются распространенной патологией, для лечения которой разрабатывают покровные мембраны. Целью исследования было изучить морфологические особенности регенерации слизистой оболочки рта при применении полимерных пьезоэлектрических мембран. Исследование проведено на 45 крысах Wistar, разделенных на группы: 1) животные с открытым раневым дефектом; 2) животные с раневым дефектом, перекрытым полимерной мембраной с медным напылением; 3) интактные животные. Забор материала для морфометрического исследования проводили на 3-и, 7-е и 12-е сутки. На 3-и сутки в группе 1 удельная площадь грануляционной ткани была в 1,4 раза больше, чем в группе 2 ($p = 0,033$). Эндотелиоциты ее сосудов экспрессировали VEGF в большей степени в группе 2. В группе 2 происходило полное перекрытие дефекта эпителиальным пластом в отличие от группы 1. На 7-е сутки в группе 2 эпителий был в 2 раза толще, чем в группе 1 ($p = 0,019$). Грануляционная ткань замещалась рыхлой волокнистой соединительной тканью. В группе 1 преобладала удельная площадь воспалительной инфильтрации над рыхлой волокнистой соединительной тканью, экспрессия VEGF была ниже, чем в группе 2. На 12-е сутки в группе 2 преобладала рыхлая волокнистая соединительная ткань, экспрессия VEGF не отличалась от группы 3, отмечалось прорастание периферических нервов. В группе 1 удельная площадь плотной волокнистой ткани была в 3,9 раз больше, чем в группе 2 ($p = 0.012$), в эпителии имелись патологические изменения, а экспрессия VEGF была ниже контрольных значений. Таким образом, использование полимерной пьезоэлектрической мембраны благоприятно влияло на восстановление тканей слизистой оболочки полости рта в области раневого дефекта.

Ключевые слова: регенерация, раневой дефект, скаффолды, пьезоэлектрики, слизистая оболочка полости рта, воспаление

Финансирование: исследование выполнено при финансовой поддержке РФФ в рамках научного проекта №23-25-00346.

Вклад авторов: А. Д. Коняева, Е. Ю. Варакута, Е. Н. Больбасов, К. С. Станкевич — концепция и дизайн исследования; А. Д. Коняева, А. Е. Лейман — сбор и обработка материала; А. Д. Коняева, Е. Ю. Варакута, Д. О. Рафиев — написание текста; А. Д. Коняева, Е. Ю. Варакута, Д. О. Рафиев, Е. Н. Больбасов, К. С. Станкевич — редактирование текста.

Соблюдение этических стандартов: исследование одобрено этическим комитетом Сибирского государственного медицинского университета (№ 7693/1 от 26 августа 2019 г.). Все манипуляции с животными проводили в соответствии с директивой Европейского Парламента № 2010/63/EU от 22.09.2010 «О защите животных, используемых для научных целей» и Хельсинской декларацией.

✉ **Для корреспонденции:** Анастасия Денисовна Коняева
Московский тракт, д. 2, г. Томск, 634034, Россия; asyakonya95@gmail.com

Статья получена: 18.05.2023 **Статья принята к печати:** 02.06.2023 **Опубликована онлайн:** 19.06.2023

DOI: 10.24075/vrgmu.2023.020

Regeneration of a wound defect is a complex process that involves interaction of epithelium, trophic apparatus, fibroblasts, and inflammatory infiltration [1]. Healing includes stages of inflammation, regeneration and reorganization; at each of these stages, the mentioned interacting components have their own morphological scar features [2]. Primary intention healing requires the fastest possible transition from the stage of inflammation to the regeneration stage. Secondary intention healing, which results in a scar, typically has the inflammatory stage dominating the process [3].

The current approach to management of the oral mucosa wound defects implies use of covering materials that protect the wound surface from re-traumatization, which adds urgency to the task of developing new wound dressings that will not only protect the wound but also reduce the severity of inflammation and accelerate regeneration [4].

The polymer piezoelectric membrane tested in the context of this study was made in the Laboratory of Hybrid Materials of the National Research Tomsk Polytechnic University. In addition to piezoelectric properties, it was modified with copper ions, which have proven antimicrobial and anti-inflammatory properties [5].

The purpose of this study was to explore morphological features of regeneration of oral mucosa with an experimental wound covered with polymer piezoelectric membranes.

METHODS

The experiment involved 45 male Wistar rats bred in the vivarium of the Central Research Laboratory of the Siberian State Medical University. The animals were kept under standard vivarium conditions; their rations were limited for a day post surgery. The rats were divided into three groups: group 1, experimental ($n = 15$), in which the animals had the wound defect left open as prescribed by the standard oral cavity wound treatment protocol; group 2, experimental ($n = 15$), where the wound defect was covered with a copper-modified polymer membrane based on vinylidene fluoride with tetrafluoroethylene; group 3, control ($n = 15$), comprised of rats with intact mucosa. The animals were kept under standard vivarium conditions.

Before wound infliction, the animals received 0.3 mg Zoletil intramuscularly that induced narcosis. After sanitizing the surgical field with a 2% chlorhexidine solution, we excised a 7–4 mm buccal mucosa flap. Next, a polymer membrane was stitched onto the resulting wound with simple interrupted sutures along the edge.

The animals were withdrawn from the experiment through hypoxia in a CO₂ chamber on the 3rd, 7th, and 12th days of the study. After withdrawal, we excised buccal mucosa at the wound defect site.

Preparation of histological specimens followed the generally accepted routine; the slides were examined in the Observer D1 light microscope (Karl Zeuss; Germany) with the AxioCam ICc5 camera (Karl Zeuss; Germany). For the purpose, after deparaffinization, the sections were stained with hematoxylin-eosin as per the standard procedure.

For immunohistochemistry, we deparaffinized the previously prepared serial paraffin sections 4–6 μm thick and then stained them with rabbit recombinant polyclonal VEGF antibodies and IgG isotype S-100 (Abcam; USA). The intensity of immunohistochemical staining was assessed on a four-point scale: 0 — no staining, 1 — weak staining, 2 — moderate staining, 3 — strong staining, 4 — very strong staining.

The calculation formula was as follows:

$$\text{Histochemical index (H-score)} = \sum P(i) \times i,$$

where i is the intensity of staining in points from 0 to 4, $P(i)$ — percentage of differently stained cells (by intensity of staining).

We did the counting in three cohorts of 100 cells in different fields of view (lens $\times 40$).

To examine the samples with an electron microscope, we put them in a 2.5% glutaraldehyde solution on the 0.2 M cacodylate buffer (1:9) for fixation and then postfixed the samples in a 1% OsO₄ solution in a refrigerator for 4 hours. The next steps involved dehydration and pouring into a mixture of epon and araldite M.

Ultrathin slides were prepared in the LKB-5 ultratome (BROMMA; Sweden), counterstained with uranyl acetate and lead citrate, and examined using a JEM-1400 CX electron microscope (JEOL; Japan).

Morphometry was performed based on the classical methods of stereometry. We established the thickness of the epithelial layer, the quantitative density of fibroblasts, the specific area of loose and dense fibrous connective tissue, that of granulation tissue and inflammatory infiltration. The software used for the purpose was the Axio Vision imaging system (Karl Zeuss; Germany) and ImageJ, version 1.52u (National Institute of Public Health; USA).

Ultrathin slides allowed us to study ultrastructure of the cells of epithelial layer, trophic apparatus, and fibroblasts.

The data were processed with Statistica 10.0 (IBM; USA). To verify distribution in the statistical hypotheses, we used the Kolmogorov–Smirnov test. The results were processed with the help of methods of descriptive and nonparametric statistics. The studied parameters were described as a median and quartiles, $M (Q_1; Q_3)$. Comparing independent samples, we used the Kruskal-Wallis test with a median test, for paired comparisons — Wilcoxon test. The differences were considered significant at $p < 0.05$.

RESULTS

On the 3rd day of the study, we registered marginal epithelialization of the wound in experimental group 1 was observed, while in group 2 the defect was completely covered by the epithelium, and there were acantholytic blisters there (Fig. 1A).

At the ultrastructural level, samples from both groups had elongated width-wise basal cells, and it was not possible to identify the apical-basal polarity. In group 2, there were signs of high proliferative activity, and some cells were undergoing mitosis (Fig. 1B).

We discovered a regeneration area filled with granulation tissue with numerous thin-walled vessels (Fig. 1C). The specific area of granulation tissue in the experimental group 2 was 1.4 times higher than in the experimental group 1, the difference being significant ($p = 0.033$) (see Table). There was an extensive zone of inflammatory cell infiltration separating healthy tissues from the wound defect; in group 2, it was 1.4 times smaller than in group 1, this difference being significant, too ($p = 0.017$). The said zone consisted of neutrophils, macrophages, plasma cells, lymphocytes, and eosinophils (see Table) (Fig. 1D).

Quantitatively, there were significantly more fibroblasts per 1 mm² of the section in group 2 ($p = 0.035$) (see Table). In addition, separate bundles of connective tissue fibers were found in the animals of this group (Fig. 1A).

We discovered newly formed thin-walled granulation tissue vessels in the area of the wound defect; their endotheliocytes actively expressed VEGF (Fig. 1E), and the calculated H-score in group 2 was 1.4 and 4.7 times higher (significant difference) than in groups 1 and 3 ($p = 0.029$, $p = 0.019$) (see Table).

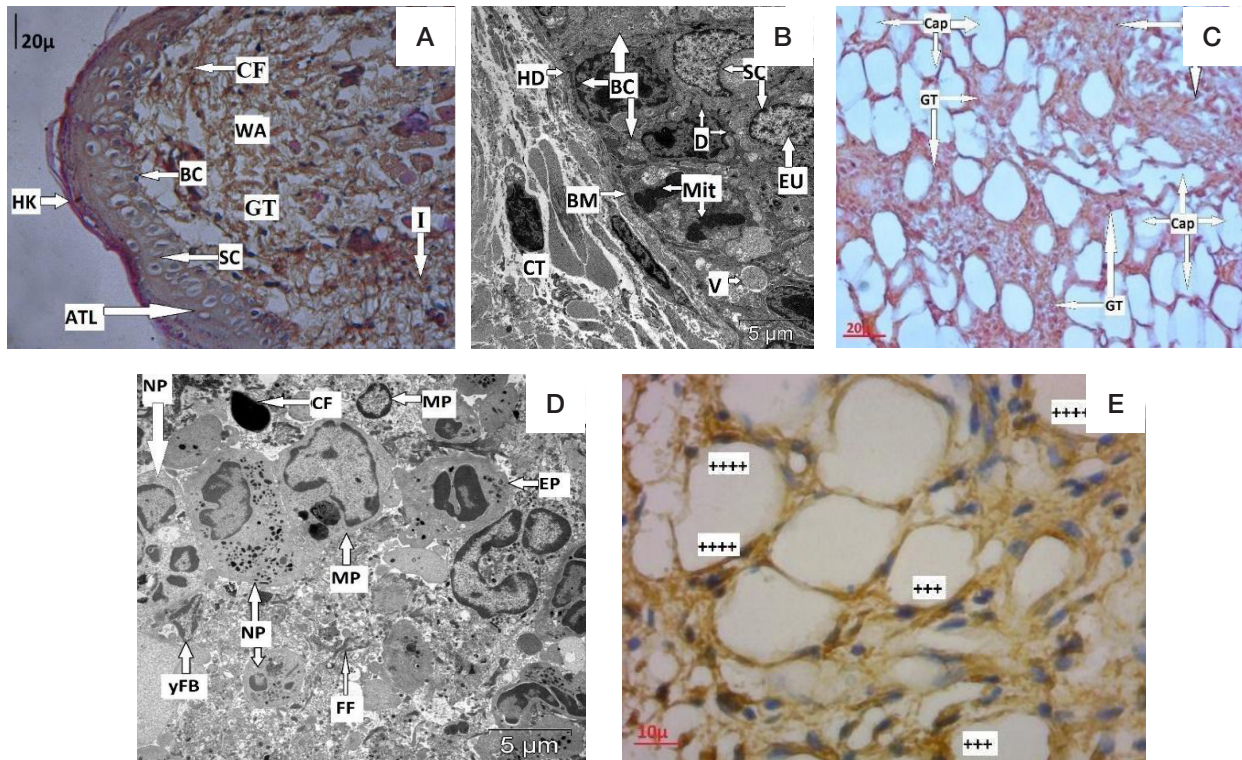


Fig. 1. Rat's buccal mucosa after infliction of the experimental wound defect, 3rd day of the study. **A.** Newly formed thin epithelial layer in the area of the wound defect and underlying granulation tissue. Pathological changes (acantholysis). Experimental group 2, 3rd day of the study (staining: hematoxylin, eosin; magnification: 400). **B.** Basal layer cells with signs of intense proliferation and mitotic figures. Experimental group 2, 3rd day of the study (TEM; magnification: 5000). **C.** New vessels in granulation tissue. Histological picture seen in both experimental groups. Experimental group 2, 3rd day of the study (staining: hematoxylin, eosin; magnification: 400). **D.** Cellular infiltration in the area of the wound defect. Histological picture seen in both experimental groups. Experimental group 1, 3rd day of the study (TEM; magnification: 5000). **E.** Expression of VEGF in the endotheliocytes of granulation tissue; nuclei stained with hematoxylin. Experimental group 2, 3rd day of the study (magnification: 900)

Endothelial lining and basement membrane of the granulation tissue capillaries were thin, and the interendothelial spaces were enlarged. The endotheliocytes were poor in organelles. In group 2, we identified a large number of micropinocytic vesicles and numerous microvilli in the endotheliocytes near the luminal edge of the vessels.

On the 7th day of the study, epithelium completely covered the wound defect in both experimental groups. The thickness of the epithelial layer in group 1 was significantly lower than that in groups 3 and 2 (see Table); there were clear active acantholytic processes (Fig. 2A).

In group 2, epithelium had less pronounced pathological changes than in group 1. The surface began to assume a typical relief with papillae, yet there still were spots of acanthosis and acantholysis. The epithelium was 2.3 times less thick than in the control group (significant difference, $p = 0.023$) but twice as thick as in group 1, where the animals had no membranes covering the defect (significant difference, $p = 0.019$) (see Table). Basal cells gradually assumed the typical shape elongated height-wise and apical-basal polarity, and there appeared hemidesmosomes restoring contacts with the basement membrane.

In both experimental groups, spots of loose fibrous connective tissue were identified in the lamina propria of buccal mucosa by the wound. In group 2, the specific area thereof was 4.5 times greater (significant difference, $p = 0.041$) than in group 1, but 2.6 times smaller than in the control group (significant difference, $p = 0.034$).

In the experimental group 2, the quantitative density of fibroblasts was 1.35 times higher than in the experimental group 1 ($p = 0.041$). Also, the prevailing type of fibroblasts in group 2 were the large differentiated branched fibroblasts

with high synthetic activity. Their plasma membrane sprouted numerous outgrowths. Bundles of connective tissue fibers in different planes were found around the cells (Fig. 2B). As for group 1, there still prevailed young fibroblasts with ultrastructure practically unchanged since the 3rd day of the experiment.

The newly formed vessels in group 2 had the VEGF expression 1.7 and 3.6 times higher than in group 1 and in the control group, respectively (significant difference, $p = 0.022$ and $p = 0.015$) (see table).

At the ultrastructural level, endotheliocytes in group 1 still showed signs of transcapillary metabolism disorders, which was not registered in the experimental group 2 (Fig. 2B), where the basement membrane of the vessels became continuous and uniform in thickness.

In both experimental groups, we discovered peripheral nerves near blood vessels by the wound defect's limits, the dendrons thereof having single edematous mitochondria with destruction of cristae. As shown on Fig. 2D, perineural and endoneurial space were edematous (Fig. 2D).

On the 12th day of the study, the animals of group 2 had the epithelial layer as thick as it originally was, while in group 1 that layer was significantly thinner than when the mucosa was intact (see Table). There were no pathological processes registered in the epithelium in group 2, and the underlying connective tissue protruded into the epithelium forming pronounced papillae with microvasculature vessels (Fig. 3A). In group 1, on the contrary, we saw signs of acantholysis, which, at the ultrastructural level, caused appearance of vacuoles in the intercellular space and, with cells proliferating, acanthosis in the spinous layer (Fig. 3B).

On the 12th day of the study, granulation tissue was replaced with young loose fibrous connective tissue in both

Table. Morphological indicators of changes in the oral mucosa during regeneration of a wound defect, M (Q₁:Q₃)

	Epithelium thickness, μ	Numerical density of fibroblasts, c.u.	Specific area of granulation tissue, %	Specific area of loose connective tissue, %	Specific area of fibrous connective tissue, %	Specific area of inflammation infiltration, %	VEGF
Control	203.9 (200.2; 204.4)	380.0 (376.0; 391.7)	–	92.3 (87.2; 95.4)	–	7.7 (5.2; 9.5)	80.0 (75.0; 85.0)
Day 3							
Group 1	–	3782.0* (3721.0; 3849.5)	43.4 (39.4; 47.9)*	–	–	56.6 (50.3; 60.9)*	275.0 (265.0; 290.0)*
Group 2	20.3 (19.1; 22.1)*	5378.5** (5346.2; 5465.7)	60.8 (58.5; 62.6)**	–	–	39.2 (37.3; 41.4)**	375.0 (370.0; 380.0)**
Day 7							
Group 1	44.5 (43.2; 6.1)*	4530.5* (4472.5; 4579.7)	38.9 (35.8; 41.8)*	7.8 (6.3; 9.1)*	–	52.8 (49.9; 56.6)*	165.0 (155.0; 175.0)*
Group 2	87.8 (85.7; 89.5)**	6136.0*# (6126.0; 6145.0)†	41.6 (40.5; 43.5)*	35.1 (33.9; 35.9)**	–	23.3 (21.9; 24.1)**	275.0 (362.5; 282.5)**
Day 12							
Group 1	107.3 (106.2; 69.8)*	2746.5* (2639.0; 2906.0)	–	60.4 (52.5; 73.0)*	23.0 (14.3; 27.8)*	15.4 (11.4; 18.7)*	55.0 (55.0; 60.0)*
Group 2	184.6 (183.4; 1856.0)#	397.5# (395.0; 402.0)	–	92.7 (92.5; 93.9)#	5.9 (5.5; 6.3)**	1.4 (1.2; 1.9)**	120.0 (125.0; 135.0)**

Note: * — significant differences compared to the control group ($p < 0,05$); # — significant differences compared to group 1 ($p < 0,05$).

experimental groups (Fig. 3A). However, the specific area of this tissues reached the control value thresholds only in the experimental group 2. In group 1, we found interstitial edema between connective tissue fibers, and there were cicatricial foci based on the dense fibrous connective tissue (Fig. 3B). Table below shows the values; the maximum specific area of such connective tissue was registered in the experimental group 1.

The quantitative density of fibroblasts in group 2 equaled the respective control value; it was 6.9 times smaller than in group 1 (significant difference, $p = 0.032$). The predominant cells in group 2 were fibrocytes, mature and functionally inactive. There was no extracellular edema around them, but the clearly organized collagen fibers were easily identifiable. At the considered time point, the predominant cells in group 1 were still the branched cells with developed synthesis organelles and dispersed chromatin.

In the experimental group 2 we registered mature, well-formed microvasculature vessels with no signs of sludge, stasis, and thrombosis. The vessels were surrounded with structured connective tissue fibers; there was no perivascular edema. The basement membrane was continuous, of uniform thickness. The quantity of organelles was sufficient, they had a typical structure. There was an active transcapillary exchange under way. In group 1, the capillary basement membrane was thin; we registered few microvilli and micropinocytic vesicles at endotheliocytes, with clearly seen perivascular edema.

Compared to the indicators recorded on the 7th day, expression of the VEGF decreased in both experimental groups. In the experimental group 1, the VEGF H-score was 1.45 times smaller than the control values ($p = 0.026$) (Fig. 3C, D).

Peripheral nerves with unmyelinated nerve fibers in wound defect area were registered only in the experimental group 2 (Fig. 3D). Despite this, immunohistochemistry did not reveal expression of the S-100 marker, which the indicated the nerves began to restore (Fig. 3E).

DISCUSSION

With this study, we have demonstrated the key morphological aspects of the wounded oral mucosa tissue regeneration under a copper-modified polymer piezoelectric membrane.

On the 3rd day of the experiment, in group 2, where the wound was covered with the membrane, the wound was fully covered with a thin layer of epithelium, while in group 1, the animals of which had no membrane on their wounds, only marginal epithelization was observed. The process of epithelization translated into changes at the ultrastructural level that enabled migration of epithelial cells from the wound's edges to its center [6]. Rørth reported preservation of single desmosomal contacts in his works and explained their presence by the need for coordinated collective migration of the epithelium [7].

Basal layer cells were proliferating intensively only in the experimental group 2. In group 1, we have not detected ultrastructural signs of high proliferative activity; lack of such signs on the part of the basal layer cells may be explained by the migrating cells' inability to undergo mitosis before the wound defect is completely covered by the epithelium layer caused by the decreased content of G1/S-phase cyclins and higher activity of cyclin-dependent kinase [8].

For the first three days, at the first stage of wound healing, inflammatory reaction was the predominant one. It was aimed at fencing healthy tissue from the defect (with its necrotic tissue), microorganisms and elements of primary contamination, as well as removal of these pathological products, elimination of the consequences of damage, activation of cytokines and growth factors [9]. In this connection, the specific area of inflammatory infiltration increased in both experimental groups.

In parallel with the inflammatory response there appeared new granulation tissue pierced with many vessels. In the experimental group 2, with the wound dressed, the ratio of the specific area of granulation tissue and inflammatory infiltration shifted towards the first component thereof, while in group 1, where the animals had no cover on the defects, the ratio prevalence was the opposite, which indicated predominance of inflammatory processes over regenerative ones.

The development of granulation tissue ensured rejection of the dead substrate, created a barrier preventing the spread of microorganisms, and formed the basis for new connective tissue developing at subsequent stages of wound regeneration [10].

Neovascularization was the basic mechanism of wound healing [11]. Capillaries were forming actively in the granulation tissue in

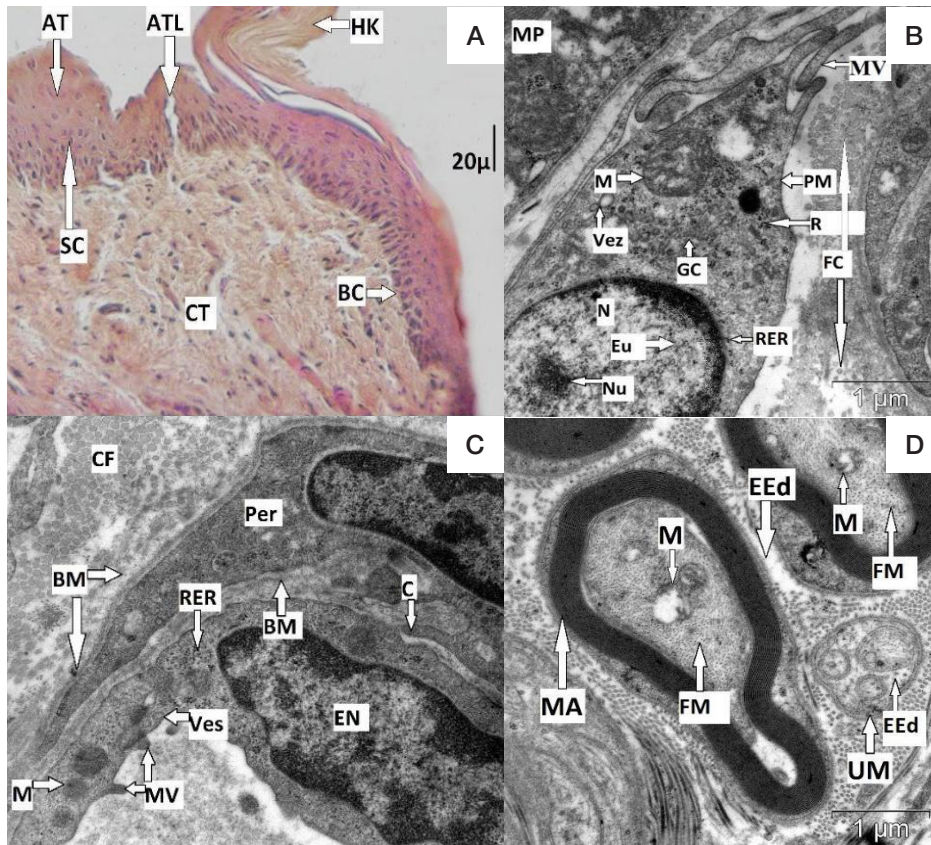


Fig. 2. CRat's buccal mucosa after infliction of the experimental wound defect, 7th day of the study. **A.** Pathological changes in the epithelium, wound defect in the process of regeneration: unevenly thick epithelial layer, thick spinous layer, acantholysis. Experimental group 1, 7th day of the study (staining: hematoxylin, eosin; magnification: 400). **B.** Differentiated fibroblast surrounded by connective tissue fibers, wound defect area. Experimental group 2, 7th day of the study (TEM; magnification: 20000). **C.** Interdigitation between an endothelial cell and a capillary pericyte, wound defect site. Experimental group 2 (TEM; magnification: 20,000). **D.** Peripheral nerve with myelinated and unmyelinated fibers, showing signs of perineural and endoneurial edema. Experimental group 2, 7th day of the study (TEM; magnification: 20000).

both experimental groups. Neoangiogenesis and inflammatory response stimulated endothelium and the inflammatory infiltrate cells to express pro-angiogenic molecules — vascular endothelial growth factor (VEGF) and chemokines needed for capillary growth. Previously, researchers have noted that VEGF in the area of a wound defect undergoing regeneration supported the inflammatory response and increased vascular permeability, which contributed to the swelling of the surrounding tissues [12]. In our study, the expression of VEGF was increasing in both experimental groups, especially in group 2, which signaled of a more intense vascularization in the absence of exposure to aggressive factors present in the oral cavity.

On the 7th day of the study, proliferation became the dominant process, with fibroblasts responsible for collagen synthesis and reduction of the wound area playing the key role therein [13]. Fibroblasts secreted an extracellular matrix replacing the fibrin matrix [14], which boosted the synthesis, as registered at the ultrastructural level in the experimental group 2. Their presence in the wound defect area was connected with a significant increase of the specific area of loose fibrous connective tissue in comparison with experimental group 1, where, according to the TEM data, young fibroblasts with low synthetic activity mainly appeared.

On the 7th day of the experiment, the specific area of granulation tissue decreased, and the newly formed vessels underwent changes at the ultrastructural level, as evidenced by the results of immunohistochemistry. The expression VEGF decreased in group 1 significantly more than in group 2, which subsequently hindered blood supply in the wound defect area [15].

The characteristic features of the proliferation stage were differentiation of epithelial cells and thickening of layers of the

epithelium. At the ultrastructural level, in group 2, the apical-basal polarity of the basal layer, desmosomal contacts between cells, and hemidesmosomes with the basement membrane were restoring. We have also seen signs of acceleration of proliferation. In both experimental groups, there were registered pathological changes in the form of acanthosis and acantholysis; morphologically, they manifested as tissue detritus in the intercellular space and thickening of the spinous layer. These pathological features were more pronounced in group 2.

Cicatricial reorganization was the next stage of wound regeneration; it occurred on the 12th day of the study. In contrast with the experimental group 1, in group 2 the specific area of loose fibrous connective tissue was greater than that of scar tissue, and the predominant cells there were the synthetically inactive fibrocytes.

In both experimental groups the number of microvasculature vessels decreased on the 12th day. Previous reports link this regression to selective apoptosis happening against the background of the increasing production of antiangiogenic factors and decreasing expression of proangiogenic factors, such as VEGF [12]. As a confirmation of these findings, in the experimental group 1 we observed that VEGF expression was significantly lower than peculiar to intact mucosa. This signaled of poor blood supply at the wound defect site, which is one of the main causes of cicatricial deformity [16]. In group 2, the expression of vascular markers was higher than the control values.

Using an electron microscope, on the 12th day of the study we saw peripheral nerves with unmyelinated nerve fibers in the experimental group 2; while such were not found in group 1, there, along the edges of the wound defect, we discovered peripheral nerves with signs of perineural and endoneurial edema

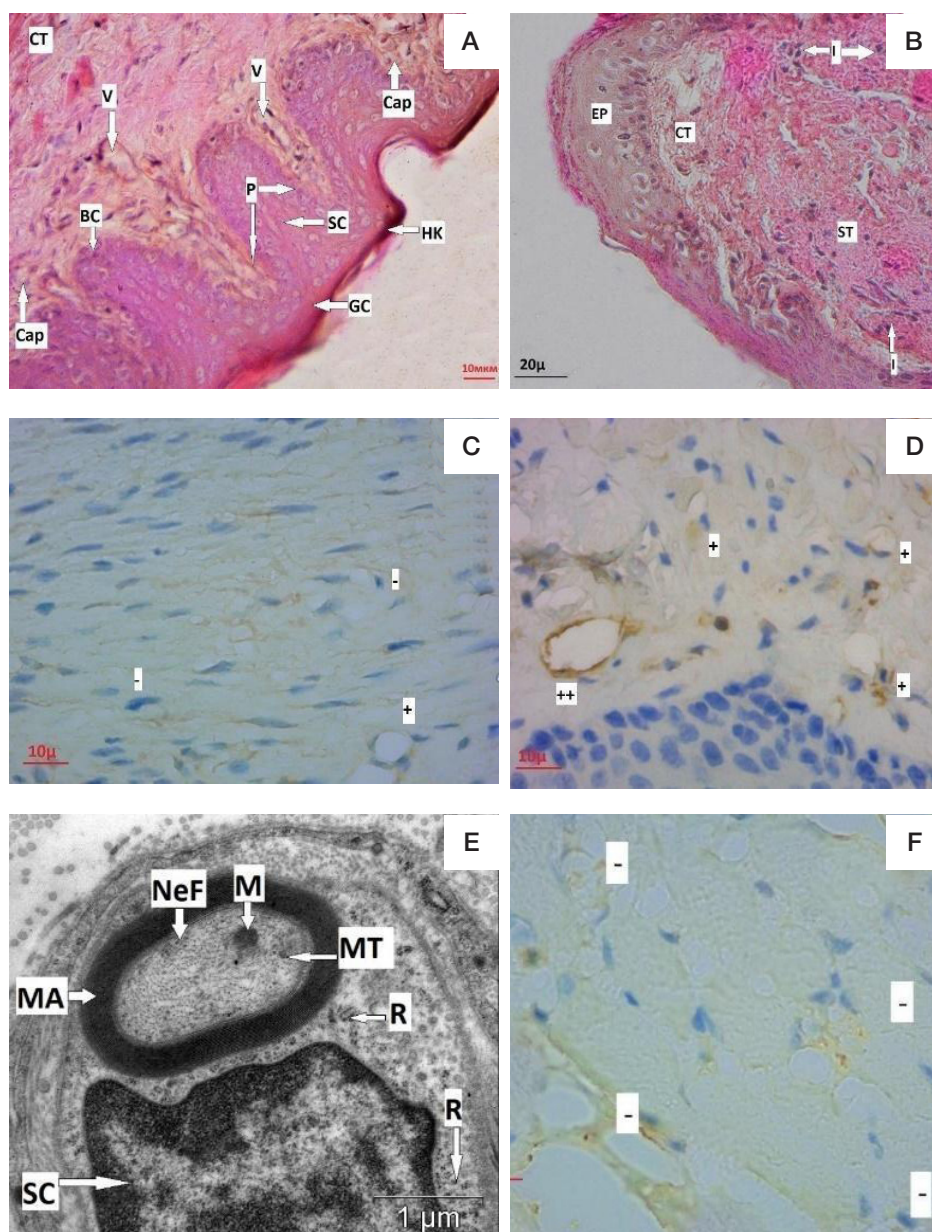


Fig. 3. Rat's buccal mucosa after infliction of the experimental wound defect, 12th day of the study. **A.** Restored mucosa. Experimental group 2, 12th day of the study (staining: hematoxylin, eosin; magnification: 400). **B.** Cicatricial tissue, wound defect site. Experimental group 1, 12th day of the study (staining: hematoxylin, eosin; magnification: 400). **D, C.** Expression of VEGF in the endotheliocytes of granulation tissue; nuclei stained with hematoxylin. **C.** Experimental group 1, 12th day of the study (magnification: 900). **D.** Experimental group 2, 12th day of the study (magnification: 900). **E.** Peripheral nerve with myelin fibers showing no signs of perineural and endoneural edema, wound defect area. Experimental group 2 (magnification: 20000). **F.** Absence of S-100 expression in the mucosa's lamina propria, nuclei staining with hematoxylin. Histological picture seen in both experimental groups. Experimental group 1, 12th day of the study (magnification: 900). WA — wound defect area; CT — loose fibrous connective tissue; GT — granulation tissue; ST — dense fibrous connective tissue; I — infiltration; V — venule; Cap — capillary; EP — epithelium; BM — basement membrane; BC — basal cells; SC — acanthocytes; GC — surface layer cells; HK — stratum corneum; ATL — acantholysis; AT — acanthosis; P — papillae; D — desmosomes; HD — hemidesmosomes; Va — expansion of intercellular space; PM — plasma membrane; EU — euchromatin; N — core; Nu — nucleolus; RER — granular endoplasmic reticulum; R — polysomes; M — mitochondrion; GC — Golgi complex; MV — outgrowths of plasmolemma; Vez — vesicles; C — intercellular contact; Mit — mitosis; yFB — young fibroblast; MP — macrophage; NP — neutrophil; EP — eosinophil; FC — connective tissue fibers; EN — endotheliocyte; Per — pericyte; FF — fragments of connective tissue fibers; CF — destructively altered cells; CF — collagen fibers; PN — peripheral nerve; MA — myelinated nerve fiber; UM — unmyelinated nerve fiber; PEEd — perineural space edema; EEd — edema of the endoneural space; FM — neurofilaments and microtubules; ++++ — very strong staining; +++ — strong staining; ++ — moderate staining; + — weak staining; — — no staining

the axons of which had mitochondria with destroyed cristae. The tests for expression of protein of the S-100 peripheral nerves returned negative in both groups, which indicated the nerve fibers began to grow into the wound defect area.

In the experimental group 2, where the wounds were covered with membranes, complete restoration the epithelium (both thickness and number of layers) occurred because it was protected from microorganisms. When the integrity of the epithelial layer was violated, microorganisms penetrated to the bottom of the open wound defect and excreted exotoxins

that affected the wound both from the inside and the outside, causing apoptosis of epithelial cells and disrupting their proliferation and migration, such course of events associated with collective regulation of the bacterial gene expression in the biofilm, which reinforced their resistance and ability to colonize [17]. In addition, metabolic products of microorganisms boosted production of pro-inflammatory mediators in the epitheliocytes through toll-like receptors [18]. As a result, in group 1 we saw epithelium growing thinner and losing layers, while acanthosis and acantholysis, the pathological changes, persisted.

CONCLUSIONS

The polymer membrane helped form an epithelial layer completely covering the wound defect on the 3rd day of the study and ensured absence of pathological changes on the 12th day thereof. In the group that had no such membrane, epithelization of the wound occurred only on the 7th day, and pathological changes (acanthus and acantholysis) were seen on the 12th day.

The membrane boosted replacement of granulation tissue with loose fibrous connective tissue and decreased the severity of inflammatory infiltration and cicatricial changes. In the group without membranes, by the end of the study, the wound defect

was mainly filled with dense fibrous connective tissue, and there was a pronounced inflammatory infiltration observed.

The polymer membrane boosted neoangiogenesis, which translated into a more intense expression of the VEGF (compared to the group without the membrane) registered at each time point of the study.

Overall, we have shown that use of a polymer piezoelectric membrane had a positive effect on the restoration of the oral mucosa tissues in the wound defect area, which manifested as an accelerated restoration of the epithelium, trophic apparatus and connective tissue component. Further, this helps optimize the process of treatment of wounds of this localization and improve quality of life of the patients.

References

- Hakkinen L, Koivisto L, Heino J, Larjava H. Cell and molecular biology of wound Healing. In: A. Vishwakarma, P. Sharpe, S. Shi, M. Ramalingam, editors. Stem cell biology and tissue engineering in dental sciences. Amsterdam, Boston, Heidelberg, London, New York: Elsevier, Academic Press, 2015; p. 669–90.
- Ridiandries A, Tan JTM, Bursill CA. The role of chemokines in wound healing. *Int J Mol Sci*. 2018; 19 (10): 3217. DOI: 10.3390/ijms19103217.
- Ozgok Kangal MK, Regan JP. Wound Healing. In: StatPearls [Internet]. Treasure Island (FL): StatPearls Publishing, 2023. PMID: 30571027. Available from: <https://www.ncbi.nlm.nih.gov/books/NBK535406/>.
- Zeng Q, Qi X, Shi G, Zhang M, Haick H. Wound dressing: from nanomaterials to diagnostic dressings and healing evaluations. *ACS Nano*. 2022; 16 (2): 1708–33. DOI: 10.1021/acsnano.1c08411.
- Badaraev A, Koniaeva A, Krikova SA, Shesterikov E, Bolbasov E, Nemoykina AL, et al. Piezoelectric polymer membranes with thin antibacterial coating for the regeneration of oral mucosa. *Applied Surface Science*. 2020; 504: 144068. DOI: 0.1016/j.apsusc.2019.144068.
- Marconi GD, Fonticoli L, Rajan TS, Pierdomenico SD, Trubiani O, Pizzicannella J, et al. Epithelial-mesenchymal transition (EMT): The type-2 EMT in wound healing, tissue regeneration and organ fibrosis. *Cells*. 2021; 10 (7): 1587. DOI: 10.3390/cells10071587.
- Rørth P. Collective cell migration. Annual review of cell and developmental biology. 2009; 25: 407–29. DOI: 10.1146/annurev.cellbio.042308.113231.
- Wehrhan F, Schultze-Mosgau S, Schliephake H. Salient features of the oral mucosa. In: Hom DB, Hebda PA, Gosain AK, Friedman CD, editors. Essential tissue healing of the face and neck. Shelton (CT): People's Medical Publishing House. BC Decker Inc., 2009; p. 83–99.
- Rodrigues M, Kosaric N, Bonham CA, Gurtner GC. Wound healing: a cellular perspective. *Physiol Rev*. 2019; 99 (1): 665–706. DOI: 10.1152/physrev.00067.2017.
- Velnar T, Bailey T, Smrkolj V. The wound healing process: an overview of the cellular and molecular mechanisms. *Journal of international medical researches*. 2009; 37 (5): 1528–42. DOI: 10.1177/147323000903700531.
- Veith AP, Henderson K, Spencer A, Sligar AD, Baker AB. Therapeutic strategies for enhancing angiogenesis in wound healing. *Adv Drug Deliv Rev*. 2019; 146: 97–125. DOI: 10.1016/j.addr.2018.09.010.
- Koniaeva AD, Varakuta EY, Leiman AE, Bolbasov E, Stankevich K. Restoration of the microvasculature and hemodynamics in the oral mucosa wound defects area with and without a piezoelectric polymer membrane. *Clinical and experimental morphology*. 2022; 11: 56–66. DOI: 10.31088/CEM2022.11.3.56-66.
- Jiang D, Christ S, Correa-Gallegos D, Ramesh P, Kalgudde Gopal S, et al. Injury triggers fascia fibroblast collective cell migration to drive scar formation through N-cadherin. *Nat Commun*. 2020; 11 (1): 5653. DOI: 10.1038/s41467-020-19425-1.
- Rognoni E, Pisco AO, Hiratsuka T, Sipilä KH, Belmonte JM, Mobasser SA, et al. Fibroblast state switching orchestrates dermal maturation and wound healing. *Mol Syst Biol*. 2018; 14 (8): e8174. DOI: 10.15252/msb.20178174.
- Bao P, Kodra A, Tomic-Canic M, Golinko MS, Ehrlich HP, Brem H. The role of vascular endothelial growth factor in wound healing. *J Surg Res*. 2009; 153 (2): 347–58. DOI: 10.1016/j.jss.2008.04.023.
- Pardali E, Goumans MJ, ten Dijke P. Signaling by members of the TGF-beta family in vascular morphogenesis and disease. *Trends Cell Biol*. 2010; 20 (9): 556–67. DOI: 10.1016/j.tcb.2010.06.006.
- Waasdorp M, Krom BP, Bikker FJ, van Zuijlen PPM, Niessen FB, Gibbs S. The bigger picture: why oral mucosa heals better than skin. *Biomolecules*. 2021; 11 (8): 1165. DOI: 10.3390/biom11081165.
- Smith P, Martinez C. Wound healing in the oral mucosa. In: Cham LA, editor. Oral mucosa in health and disease: a concise handbook. Bergmeier-Switzerland: Springer Int. Publ. AG, 2018; p. 77–91.

Литература

- Hakkinen L, Koivisto L, Heino J, Larjava H. Cell and molecular biology of wound Healing. In: A. Vishwakarma, P. Sharpe, S. Shi, M. Ramalingam, editors. Stem cell biology and tissue engineering in dental sciences. Amsterdam, Boston, Heidelberg, London, New York: Elsevier, Academic Press, 2015; p. 669–90.
- Ridiandries A, Tan JTM, Bursill CA. The role of chemokines in wound healing. *Int J Mol Sci*. 2018; 19 (10): 3217. DOI: 10.3390/ijms19103217.
- Ozgok Kangal MK, Regan JP. Wound Healing. In: StatPearls [Internet]. Treasure Island (FL): StatPearls Publishing, 2023. PMID: 30571027. Available from: <https://www.ncbi.nlm.nih.gov/books/NBK535406/>.
- Zeng Q, Qi X, Shi G, Zhang M, Haick H. Wound dressing: from nanomaterials to diagnostic dressings and healing evaluations. *ACS Nano*. 2022; 16 (2): 1708–33. DOI: 10.1021/acsnano.1c08411.
- Badaraev A, Koniaeva A, Krikova SA, Shesterikov E, Bolbasov E, Nemoykina AL, et al. Piezoelectric polymer membranes with thin antibacterial coating for the regeneration of oral mucosa. *Applied Surface Science*. 2020; 504: 144068. DOI: 0.1016/j.apsusc.2019.144068.
- Marconi GD, Fonticoli L, Rajan TS, Pierdomenico SD, Trubiani O, Pizzicannella J, et al. Epithelial-mesenchymal transition (EMT): The type-2 EMT in wound healing, tissue regeneration and organ fibrosis. *Cells*. 2021; 10 (7): 1587. DOI: 10.3390/cells10071587.
- Rørth P. Collective cell migration. Annual review of cell and developmental biology. 2009; 25: 407–29. DOI: 10.1146/annurev.

- cellbio.042308.113231.
8. Wehrhan F, Schultze-Mosgau S, Schliephake H. Salient features of the oral mucosa. In: Hom DB, Hebda PA, Gosain AK, Friedman CD, editors. *Essential tissue healing of the face and neck*. Shelton (CT): People's Medical Publishing House. BC Decker Inc., 2009; p. 83–99.
 9. Rodrigues M, Kosaric N, Bonham CA, Gurtner GC. Wound healing: a cellular perspective. *Physiol Rev*. 2019; 99 (1): 665–706. DOI: 10.1152/physrev.00067.2017.
 10. Velnar T, Bailey T, Smrkolj V. The wound healing process: an overview of the cellular and molecular mechanisms. *Journal of international medical researches*. 2009; 37 (5): 1528–42. DOI: 10.1177/147323000903700531.
 11. Veith AP, Henderson K, Spencer A, Sligar AD, Baker AB. Therapeutic strategies for enhancing angiogenesis in wound healing. *Adv Drug Deliv Rev*. 2019; 146: 97–125. DOI: 10.1016/j.addr.2018.09.010.
 12. Koniaeva AD, Varakuta EY, Leiman AE, Bolbasov E, Stankevich K. Restoration of the microvasculature and hemodynamics in the oral mucosa wound defects area with and without a piezoelectric polymer membrane. *Clinical and experimental morphology*. 2022; 11: 56–66. DOI: 10.31088/CEM2022.11.3.56-66.
 13. Jiang D, Christ S, Correa-Gallegos D, Ramesh P, Kalgudde Gopal S, et al. Injury triggers fascia fibroblast collective cell migration to drive scar formation through N-cadherin. *Nat Commun*. 2020; 11 (1): 5653. DOI: 10.1038/s41467-020-19425-1.
 14. Rognoni E, Pisco AO, Hiratsuka T, Sipilä KH, Belmonte JM, Mobasser SA, et al. Fibroblast state switching orchestrates dermal maturation and wound healing. *Mol Syst Biol*. 2018; 14 (8): e8174. DOI: 10.15252/msb.20178174.
 15. Bao P, Kodra A, Tomic-Canic M, Golinko MS, Ehrlich HP, Brem H. The role of vascular endothelial growth factor in wound healing. *J Surg Res*. 2009; 153 (2): 347–58. DOI: 10.1016/j.jss.2008.04.023.
 16. Pardali E, Goumans MJ, ten Dijke P. Signaling by members of the TGF-beta family in vascular morphogenesis and disease. *Trends Cell Biol*. 2010; 20 (9): 556–67. DOI: 10.1016/j.tcb.2010.06.006.
 17. Waasdorp M, Krom BP, Bikker FJ, van Zuijlen PPM, Niessen FB, Gibbs S. The bigger picture: why oral mucosa heals better than skin. *Biomolecules*. 2021; 11 (8): 1165. DOI: 10.3390/biom11081165.
 18. Smith P, Martinez C. Wound healing in the oral mucosa. In: Cham LA, editor. *Oral mucosa in health and disease: a concise handbook*. Bergmeier–Switzerland: Springer Int. Publ. AG, 2018; p. 77–91.